

# Anisotropic-ray-theory geodesic deviation and two-point ray tracing through a split intersection singularity

Petr Bulant & Luděk Klimeš

*Department of Geophysics, Faculty of Mathematics and Physics, Charles University in Prague, Ke Karlovu 3, 121 16 Praha 2, Czech Republic,  
<http://sw3d.cz/staff/bulant.htm>, <http://sw3d.cz/staff/klimes.htm>*

## Summary

We demonstrate the principal problems with tracing the anisotropic-ray-theory S-wave rays. While the initial-value rays can safely be traced by solving Hamilton's equations of rays, it is often impossible to determine the coefficients of the equations of geodesic deviation (paraxial ray equations, dynamic ray tracing equations) and to solve them numerically. As the result, we often know neither the matrix of geometrical spreading nor the phase shift due to caustics. We show how surprisingly large is the number of rays which cannot be correctly calculated in the velocity model with a split intersection singularity.

## Keywords

Wave propagation, elastic anisotropy, heterogeneous media, anisotropic ray theory, geodesic deviation, KMAH index, two-point ray tracing, S-wave singularities.

## 1. Introduction

In a generally anisotropic medium, the S-wave slowness sheets of the slowness surface are usually mostly separated and intersect in at up to 32 point S-wave singularities (Vavryčuk, 2005a; 2005b). In this case, outside the point singularities, the anisotropic-ray-theory rays stay at the faster or slower S-wave slowness sheet, respectively. When approaching the point singularities, the limiting case again corresponds to staying at the faster or slower S-wave slowness sheet, respectively. In a generally anisotropic medium, we thus have to separate the slowness surface into the P-wave slowness sheet, the faster S-wave slowness sheet and the slower S-wave slowness sheet.

However, in a transversely isotropic medium, the S-wave slowness sheets may intersect along intersection singularities (Vavryčuk, 2003). If a medium is close to transversely isotropic but is not transversely isotropic, the intersection singularity is split, the slower S-wave slowness sheet separates from the faster S-wave slowness sheet, forming smooth but very sharp edges on both sheets.

When the slowness vector of a ray smoothly pass through a split intersection singularity or close to the vicinity of a conical or wedge singularity, the ray-velocity vector rapidly changes its direction and creates a sharp bend on the ray. This sharp bend is connected with a rapid rotation of the eigenvectors of the Christoffel matrix. The sharply bent rays thus cannot describe the correct wave propagation and indicate a failure of ray methods.

The sharply bent rays can safely be traced by solving Hamilton’s equations of rays. On the other hand, the dependence of the second derivatives of the Hamiltonian function with respect to the slowness vector along the ray contains a narrow spike resembling a Dirac distribution. This narrow spike destroys the numerical integration of the equations of geodesic deviation (paraxial ray equations, dynamic ray tracing equations), and the matrix of geometrical spreading becomes random behind the spike. Moreover the numerical integration can generate several spurious changes of the signature of the matrix of geometrical spreading, which may result in various incorrectly large KMAH indices. Random incorrect KMAH indices cannot be used for the determination of ray histories during two–point ray tracing. Even if we removed the KMAH index from ray histories, we could not use the randomly generated matrix of geometrical spreading for two–point ray tracing.

In this paper, we numerically demonstrate the problems with two–point ray tracing in velocity model SC1-II which contains a split intersection singularity.

## 2. Velocity model SC1-II

At the depth of 0 km, velocity model SC1-II is transversely isotropic with the tilted axis of symmetry. At this depth, the slowness surface contains an intersection singularity. At the depth of 1.5 km, velocity model SC1-II is very close to isotropic, but is slightly cubic and its symmetry axes coincide with the coordinate axes. This means that, at all depths except 0 km, velocity model SC1-II is very close to transversely isotropic, but is slightly tetragonal. Whereas the transversely isotropic medium contains the intersection singularity through which the rays pass without rotation of the eigenvectors of the Christoffel matrix (Vavryčuk, 2001, sec. 4.3), in the slightly tetragonal medium, the S–wave slowness surface is split at this unstable singularity (Crampin, 1981) and the eigenvectors of the Christoffel matrix rapidly rotate by  $90^\circ$  there.

## 3. Initial–value tracing of anisotropic–ray–theory S–wave rays

Previous versions of the SW3D software package CRT were designed to trace the anisotropic–ray–theory P–wave rays and the anisotropic common S–wave rays using the average S–wave Hamiltonian function according to Klimeš (2006). We did not consider anisotropic–ray–theory S–wave rays for obvious problems with S–wave slowness surface singularities. Now we have added an optional possibility to calculate anisotropic–ray–theory S–wave rays to the package CRT version 7.10 (Bucha & Bulant, 2014) for testing purposes.

Optional tracing of anisotropic–ray–theory S–wave rays is designed for general anisotropy with point S–wave singularities only. We thus a priori choose the faster S wave or the slower S wave. In each step of anisotropic–ray–theory S–wave ray tracing, the Christoffel matrix is calculated together with its eigenvalues and corresponding eigenvectors. We then select the a priori given anisotropic–ray–theory S wave (the slower one or the faster one) for the calculation of the ray.

The rays of the selected anisotropic–ray–theory S wave can safely be traced by solving Hamilton’s equations of rays. Unfortunately, the equations of geodesic deviation (paraxial ray equations, dynamic ray tracing equations) contain the second–order derivatives of the Hamiltonian function with respect to the slowness vector. Expressions for these derivatives contain the difference of the S–wave eigenvalues of

the Christoffel matrix in the denominator. If the difference of the S-wave eigenvalues of the Christoffel matrix is smaller than the rounding error, the second-order derivatives of the Hamiltonian function with respect to the slowness vector become random and, in consequence, the matrix of geometrical spreading becomes random, too. If we wish the rays with a reasonably defined matrix of geometrical spreading and a reasonably defined phase shift due to caustics, we have to terminate tracing of a ray if the relative difference between the S-wave eigenvalues of the Christoffel matrix is smaller than the prescribed limit which we named `DSWAVE`. The maximum angular numerical error of the eigenvectors of the Christoffel matrix in radians is then roughly equal to the ratio of the relative rounding error to parameter `DSWAVE`.

#### 4. Problems of two-point rays tracing in velocity model `SC1_II`

We chose the value 0.000 01 of the above mentioned parameter `DSWAVE` and traced the initial-value rays of the slower S wave. The ray parameters of the rays are displayed in Figure 1. The black plus crosses (ray history 1) correspond to the rays which do not touch a caustic and thus have the KMAH index of 0. The belt of other symbols roughly corresponds to the sharply bent rays (Klimeš & Bulant, 2014, fig. 3) which should have the KMAH index of 1. The yellow squares (ray history 4) indeed correspond to rays with the KMAH index of 1. We see that the boundary between the KMAH index of 0 and the KMAH index of 1 is not smooth, which means that the value of the KMAH index is sometimes incorrect for the chosen value of parameter `DSWAVE`. We also observe violet circles (ray history 5) corresponding to the rays with the incorrect value 2 of the KMAH index. The value 0.000 01 of parameter `DSWAVE` is thus too small for the correct determination of the matrix of geometrical spreading and of the KMAH index. On the other hand, green times crosses (ray history 2, KMAH=0) and blue diamonds (ray history 3, KMAH=1) correspond to the rays whose tracing has been terminated due to the relative difference of the S-wave eigenvalues smaller than `DSWAVE`=0.000 01. The rays whose tracing has been terminated completely cover the region of the two-point rays corresponding to the reverse branch of the wavefront triplication, refer to Figures 3 and 5, and to Klimeš & Bulant (2014, figs. 3, 4). If we wish to obtain these two-point rays, we have to considerably decrease the value of parameter `DSWAVE`, although we know, that the matrix of geometrical spreading and the KMAH index will then become random.

We thus chose the value 0.000 000 000 01 of parameter `DSWAVE` and traced the initial-value rays of the slower S wave. The ray parameters of the rays are displayed in Figure 2. The only ray whose tracing has been terminated corresponds to the violet circle (ray history 5). All other initial-value rays have been calculated, but with random values of the KMAH index. The random values of the KMAH index are 0 (ray history 1), 1 (ray history 2), 2 (ray history 3) and 4 (ray history 4).

During two-point ray tracing according to Bulant (1996; 1999), we have to determine the boundaries between the regions of different ray histories, in this case between the regions of different KMAH indices. Determination of the boundaries between the regions of random KMAH indices of Figure 2, using additional auxiliary rays with again random KMAH indices, obviously represents a disaster for the two-point ray tracing algorithm. The ray parameters of all anisotropic-ray-theory rays of the slower S wave traced with `DSWAVE`=0.000 000 000 01 during the two-point ray tracing are displayed in Figure 3 together with the triangulation of the ray-parameter domain. The random

values of the KMAH index are 0 (ray history 1), 1 (ray history 2), 2 (ray history 3), 3 (ray history 5), 4 (ray history 4), 5 (ray history 9), 6 (ray history 7) and 10 (ray history 8). Ray history 6 corresponds to the ray whose tracing has been terminated. The large red plus crosses correspond to the rays approximately leading to the receivers. The receivers are located in a vertical well at a distance of 1 km from the source. The receivers extend from the depth of 1.32 km below the source to the elevation of 0.48 km above the source with spacing of 0.04 km (Klimeš & Bulant, 2014, fig. 3).

In order to trace the anisotropic-ray-theory rays of the slower S wave in velocity model SC1\_II, we have optionally removed the KMAH index from ray histories. The ray parameters of the initial-value rays traced with  $DSWAVE=0.000\ 000\ 000\ 01$  and with the KMAH index removed from ray histories are displayed in Figure 4. In this case, the only ray whose tracing has been terminated corresponds to the green times cross (ray history 2). All other rays have been calculated and have equal ray history 1. In this way, we can find the rays approximately leading to the receivers, see Figure 5. For the pictures of ray trajectories and wavefronts refer to Klimeš & Bulant (2014, figs. 3, 4).

### Acknowledgements

The research has been supported by the Grant Agency of the Czech Republic under contract P210/10/0736, by the Ministry of Education of the Czech Republic within research projects MSM0021620860 and CzechGeo/EPOS LM2010008, and by the members of the consortium “Seismic Waves in Complex 3-D Structures” (see “<http://sw3d.cz>”).

### References

- Bucha, V. & Bulant, P. (eds.) (2014): SW3D-CD-18 (DVD-ROM). *Seismic Waves in Complex 3-D Structures*, **23**, 211–212, online at “<http://sw3d.cz>”.
- Bulant, P. (1996): Two-point ray tracing in 3-D. *Pure appl. Geophys.*, **148**, 421–447.
- Bulant, P. (1999): Two-point ray-tracing and controlled initial-value ray-tracing in 3-D heterogeneous block structures. *J. seism. Explor.*, **8**, 57–75.
- Crampin, S. (1981): A review of wave motion in anisotropic and cracked elastic-media. *Wave Motion*, **3**, 343–391.
- Klimeš, L. (2006): Common-ray tracing and dynamic ray tracing for S waves in a smooth elastic anisotropic medium. *Stud. geophys. geod.*, **50**, 449–461.
- Klimeš, L. & Bulant, P. (2014): Anisotropic-ray-theory rays in velocity model SC1\_II with a split intersection singularity. *Seismic Waves in Complex 3-D Structures*, **24**, 189–205, online at “<http://sw3d.cz>”.
- Vavryčuk, V. (2001): Ray tracing in anisotropic media with singularities. *Geophys. J. int.*, **145**, 265–276.
- Vavryčuk, V. (2003): Generation of triplications in transversely isotropic media. *Phys. Rev. B*, **68**, 054107-1–054107-8.
- Vavryčuk, V. (2005a): Acoustic axes in weak triclinic anisotropy. *Geophys. J. int.*, **163**, 629–638.
- Vavryčuk, V. (2005b): Acoustic axes in triclinic anisotropy. *J. acoust. Soc. Am.*, **118**, 647–653.

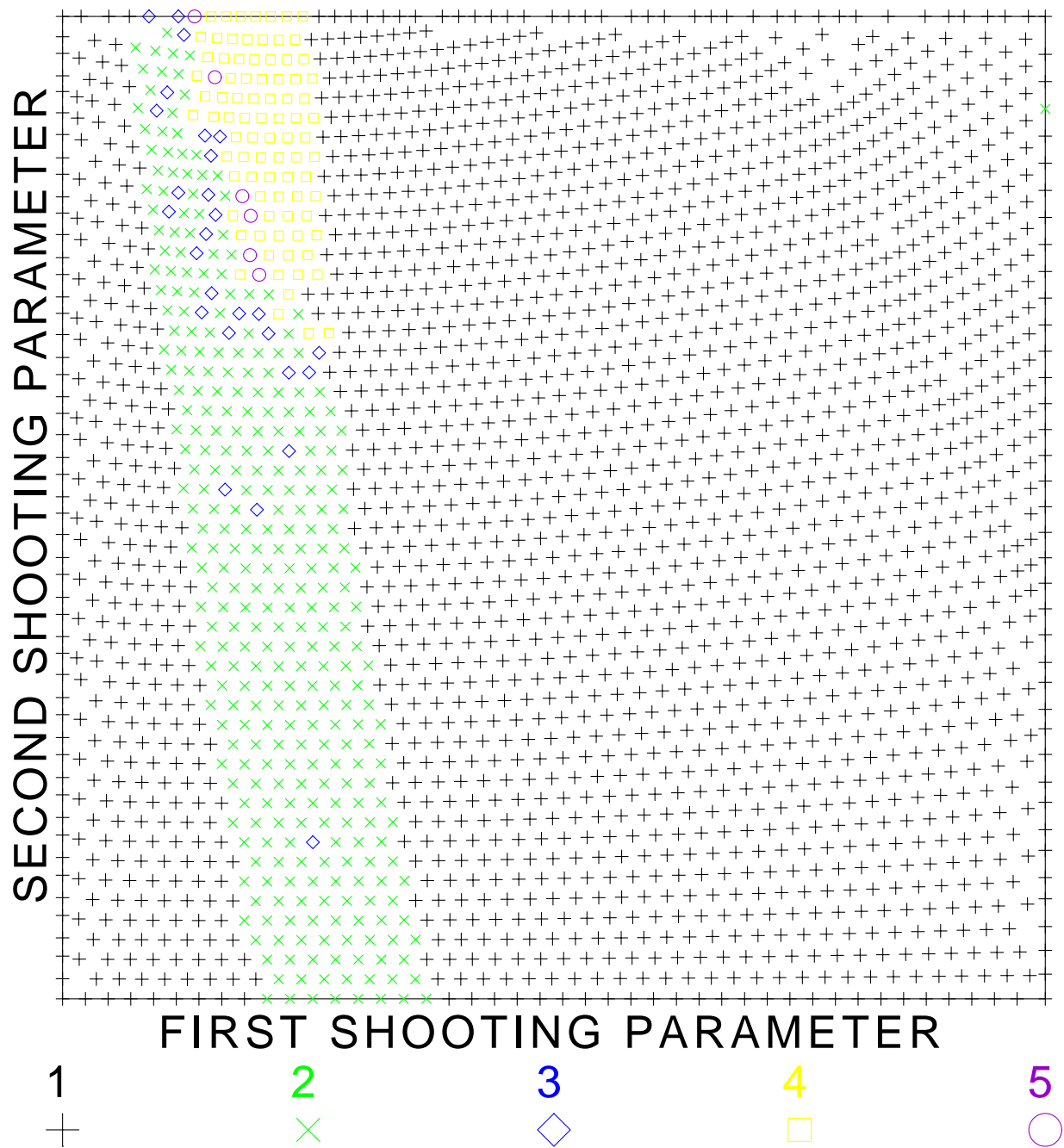


**Figure 1:** Ray parameters of the basic system of the anisotropic-ray-theory rays of the slower S wave, traced with  $DSWAVE=0.00001$  and with the KMAH index included in ray histories.

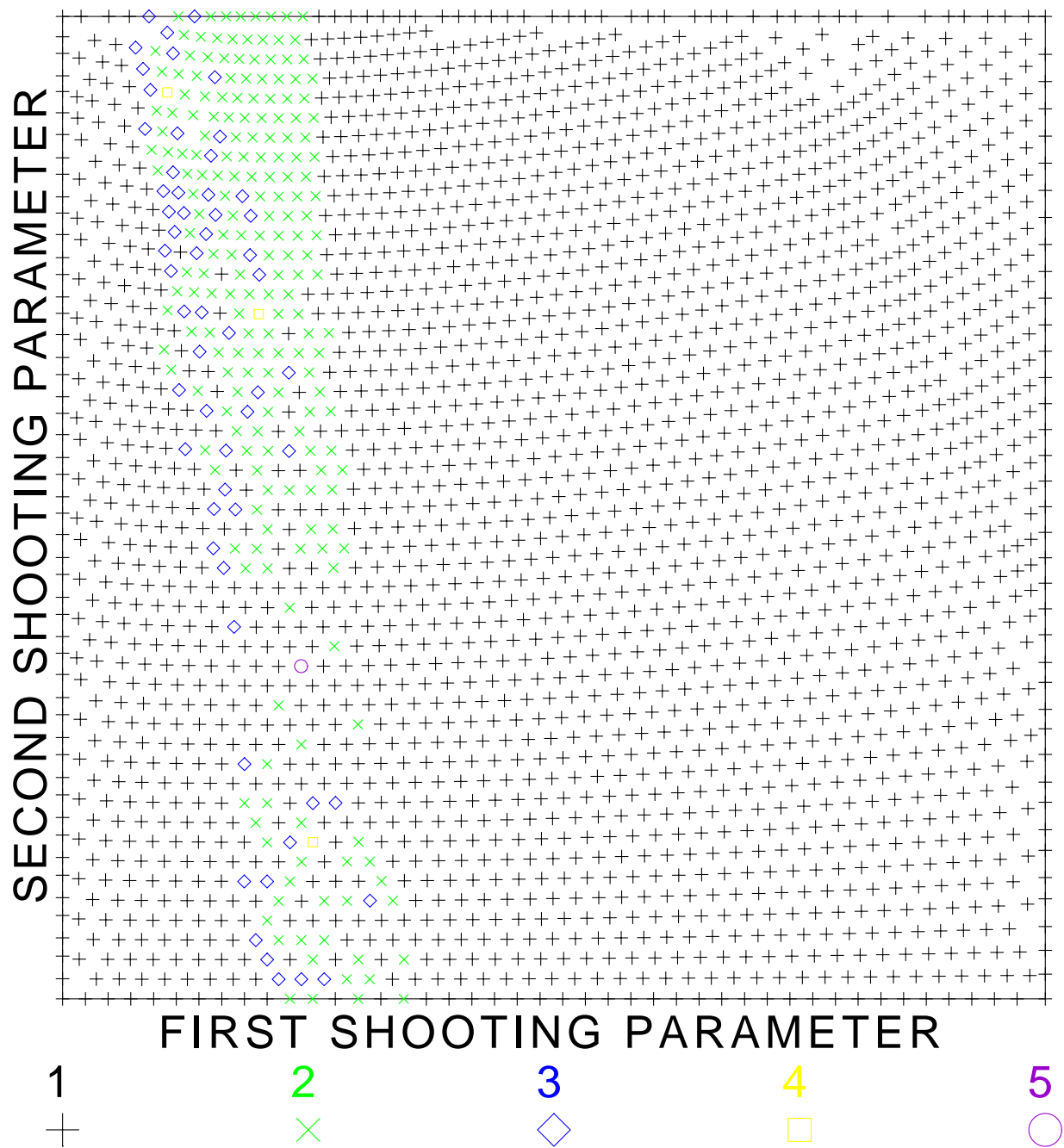


**Figure 2:** Ray parameters of the basic system of the anisotropic-ray-theory rays of the slower S wave, traced with  $DSWAVE=0.000\ 000\ 000\ 01$  and with the KMAH index included in ray histories.

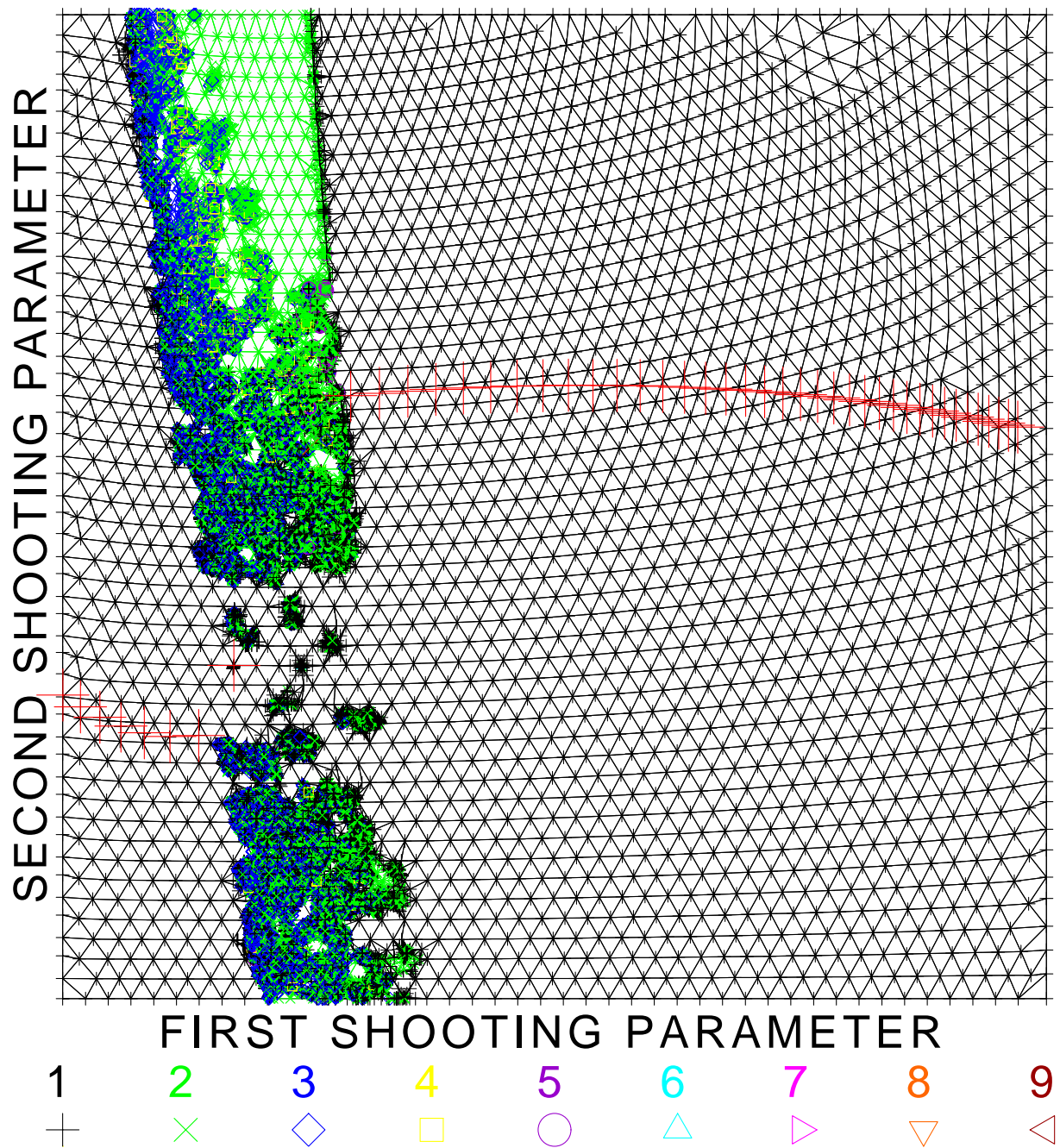


**Figure 3:** Ray parameters of all traced anisotropic-ray-theory rays of the slower S wave, including the triangulation of the ray-parameter domain. The rays are traced with  $DSWAVE=0.000\ 000\ 000\ 01$  and with the KMAH index included in ray histories. The large red crosses correspond to the rays approximately leading to the receivers.

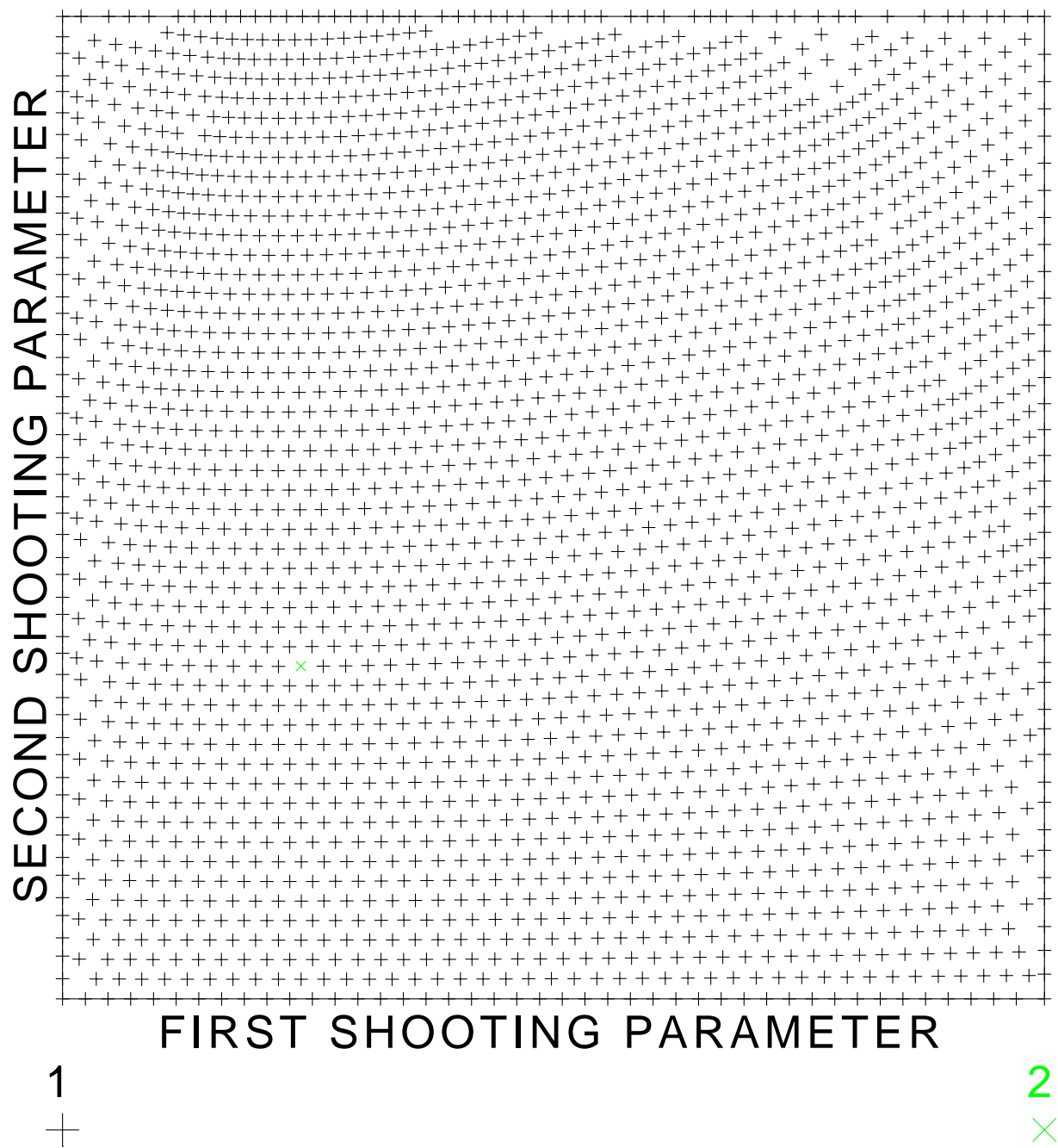


**Figure 4:** Ray parameters of the basic system of the anisotropic-ray-theory rays of the slower S wave, traced with  $DSWAVE=0.000\ 000\ 000\ 01$  and with the KMAH index removed from ray histories.

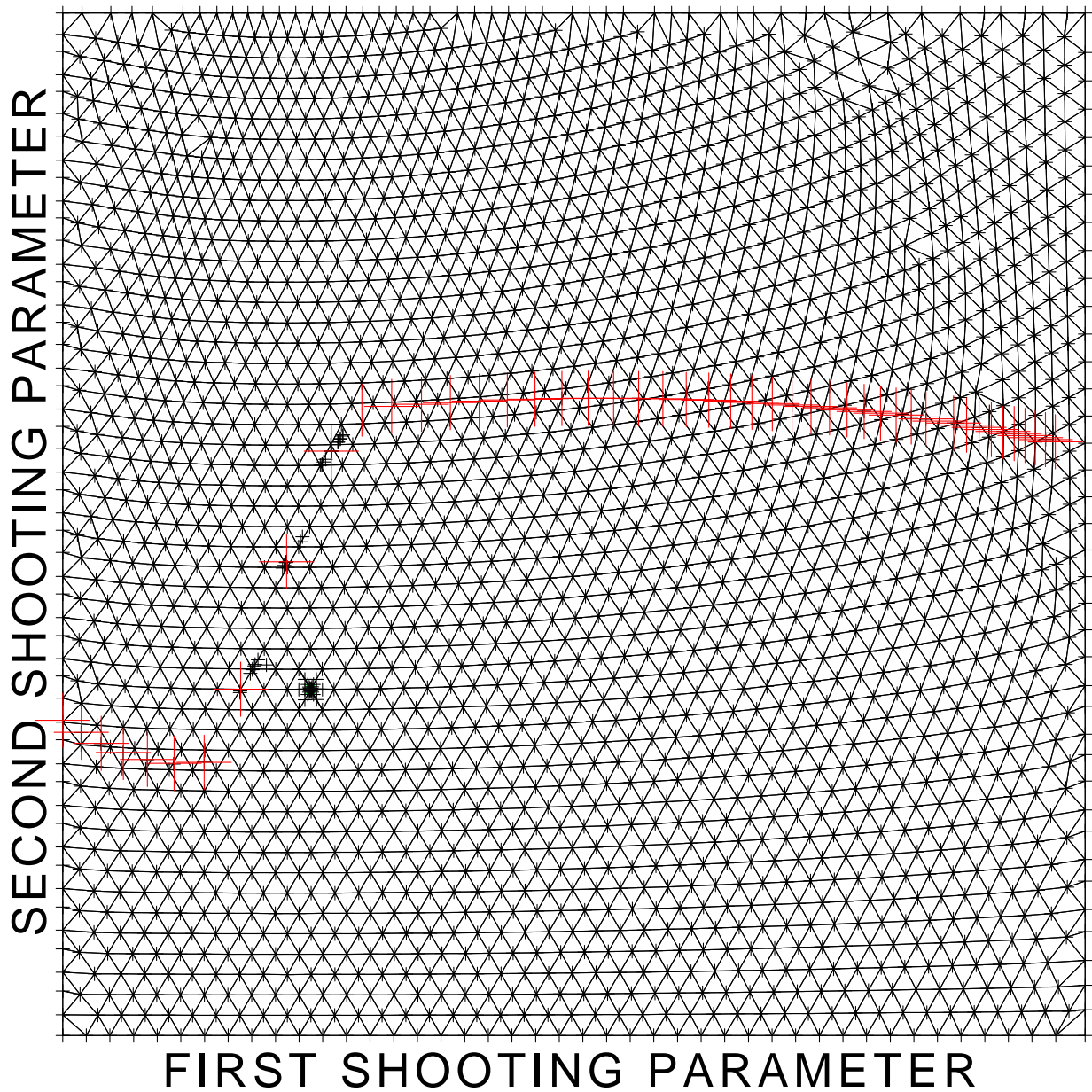


**Figure 5:** Ray parameters of all traced anisotropic-ray-theory rays of the slower S wave, including the triangulation of the ray-parameter domain. The rays are traced with  $DSWAVE=0.000\ 000\ 000\ 01$  and with the KMAH index removed from ray histories. The large red crosses correspond to the rays approximately leading to the receivers. It is obvious from the distribution of auxiliary rays shot towards the receivers that the paraxial approximation inevitably failed in the belt of sharply bent rays. The isolated cluster of auxiliary rays corresponds to the ray which could not be traced, refer to the green times cross in Figure 4.